Stress-Enhanced Chemical Vapor Deposited Graphene NEMS RF Resonators

Michael Lekas*, Sunwoo Lee*, Changyao Chen†,Wu-Joon Cha†, Karthik Ayyagari†, James Hone†, and Kenneth Shepard*
*Department of Electrical Engineering, Columbia University in the city of New York, USA
†Department of Mechanical Engineering, Columbia University in the city of New York, USA

***Abstract*—In this work we present room-temperature measurements of graphene nanoelectromechanical resonators (GNERs) demonstrating quality factors (Qs) greater than 200 at resonance. A nominal resonant frequency (f_o) of 200 MHz is attained by applying strain to the suspended graphene using an SU-8 polymer clamp. Additionally, the device f_o can be tuned by more than 5% by application of a DC gate bias on the order of 5V. Chemical vapor deposited (CVD) graphene is used to demonstrate the scalability of the process.**

I. Introduction

Graphene has received much attention owing to its exceptional electrical and mechanical properties [1], [2]. For electronic applications, graphene has been considered as a potential channel material for RF field-effect transistors (FETs) due to its high carrier mobility, saturation velocity, and current carrying capacity [3], [4]. In nano-mechanics research, graphene has been used to construct RF mechanical resonators [5], [6], [7], which take advantage of its high tensile strength,high stiffness, and low mass.

It was recently demonstrated that a graphene nanoelectromechanical resonators (GNER) can be operated as a mechanically resonant FETs to improve transduction [6], [7]. In this configuration, shown in Fig. 1, a sheet of graphene is suspended over a local metal gate electrode, and a drain-source bias (V_{ds}) is applied across the graphene. By applying both a DC voltage and an RF signal to the gate, mechanical vibrations are actuated in the graphene. Motion of the graphene relative to the gate induces a capacitive displacement current in the device (similar to that seen passive MEMS devices), as well as a current due to the field-effect modulation of channel charge. By means of this second current component, the mechanical resonance signal is sensed and amplified by the transconductance (g_m) of the graphene FET structure.

This active sensing technique creates the possibility of using graphene NEMS resonators in RF circuits such as filters and oscillators [8]. Active sensing may be especially beneficial in filtering applications since it may be used to reduce insertion loss (IL), a parameter that is especially important for maintaining an acceptable receiver noise figure.

Nonetheless, there are still obstacles to implementing GNERs in these applications, including process scalability concerns, low quality factors (Q) at room temperature, and low resonance frequencies (f_o). In this work we present measurements on GNERs that address these problems by employing a stress-enhanced design to boost f_o, and chemical vapor deposited (CVD) graphene to demonstrate the potential for wafer-level fabrication.

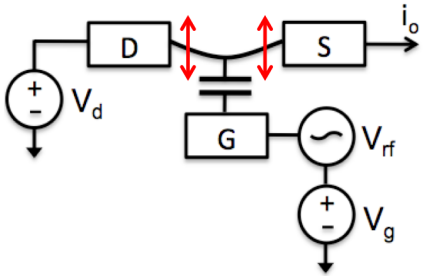

Fig. 1. Diagram showing operation of GNER.

II. Experiment

The process used to fabricate GNERs is described in detail elsewhere [9], but will be briefly outlined here. To begin, metal gates are patterned on fused silica substrates using deep-UV lithography. A layer of silicon dioxide (SiO_2) is deposited on top of the gates using plasma-enhanced chemical vapor deposition (PECVD). To improve adhesion and reduce potential wrinkling of the graphene, the oxide is chemical-mechanical polished (CMP) to reduce its roughness below 0.5 nm. CVD grown graphene is then transferred to the substrate using the technique outlined in [9].

Device channels are patterned in the graphene using electron beam lithography (EBL) and an oxygen plasma etch. Source and drain electrodes (1/15/50 nm of Ti/Pd/Au) are then patterned using EBL, and an SU-8 polymer clamp is patterned on top of the graphene in order to clamp the graphene in the shape of a drum. The sample is then hardbaked at 170C, causing the SU-8 clamp to contract and apply strain to the graphene. The devices in this work employ clamps with a circular geometry rather than a doubly-clamped structure. We find that this improves the uniformity of the strain applied to the graphene, and also serves to suppress higher-order modes that often arise in doubly clamped structures, which may adversely affect Q.

In the final fabrication step, the device is immersed in buffered oxide etchant and dried in a critical point dryer to remove the sacrificial oxide under the graphene channel and suspend the device. A scanning electron microscope (SEM) image of a finished device is shown in Fig. 2.

All measurements are conducted at room temperature in a

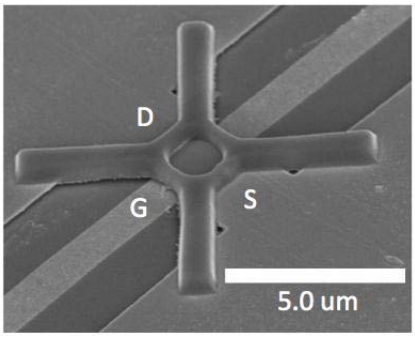

Fig. 2. SEM image of GNER.

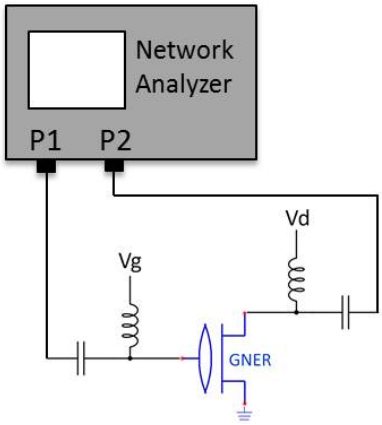

Fig. 3. RF measurement setup: gate and drain DC biases are applied through bias-T's. The input and output ports art P1 and P2, respectively.

Desert Cryogenics probe station at pressures lower than 10^{-6} torr. DC measurements are performed using an Agilent 4155c Semiconductor Parameter Analyzer. RF measurements were performed with the setup shown in Fig. 3, using an Agilent N5230A Network Analyzer.

III. Results and Discussion

Fig. 4 shows a measurement of drain current (I_{ds}) as a function of the DC gate-to-source bias (V_{gs}) for a GNER measured with a constant V_{ds}. The clamp geometry for this device is a 1.5-μm-diameter circular drum, and the graphene channel width and length underneath the clamp are 3-μm and 1.5-μm, respectively. The gate-to-channel spacing for this device is approximately 70 nm. A field-effect mobility (μ_{fe}) of 300 cm^2/V-s is calculated from these current-voltage measurements, which while lower than other data on CVD graphene samples which show mobilities as high as 40,000 cm^2/V-s [10], is sufficient to achieve g_m in excess of 15 μS. The lower mobility achieved here is most likely due to contamination of the graphene channel material during the more involved fabrication process to achieve these structures.

Fig. 5(a) shows a plot of the S_{21} magnitude for the same GNER as a function V_{gs} and frequency. Increasing V_{gs} increases the electrostatic force on the graphene, which induces additional strain in the membrane, causing f_o of the device to shift from approximately 201 MHz at 0 V to 198 MHz at 4 V. The reduction in f_o at higher V_{gs} is due to a spring softening effect that has been observed in many nanomechanical devices

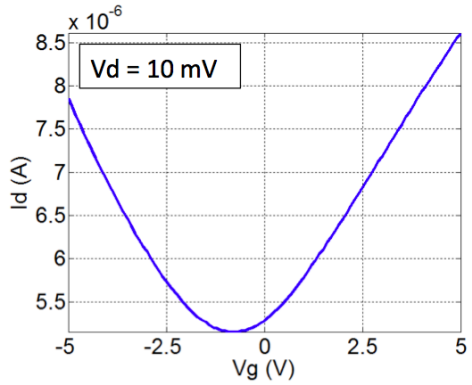

Fig. 4. Low-field transport measurement.

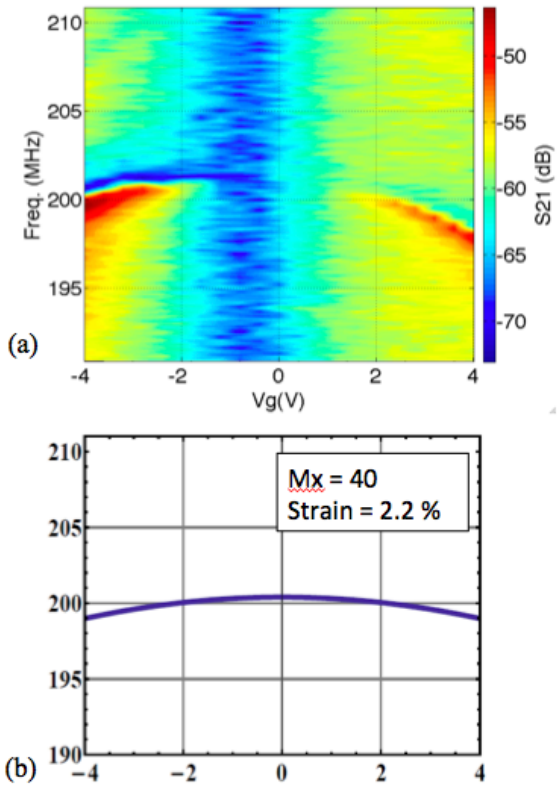

Fig. 5. (a) S_{21} magnitude as a function of frequency and V_{gs}. (b) Fitting of the resonant frequency tuning characteristic, used to extract resonator mass and strain.

[11]. Using the mechanical model for a circular membrane resonator given in [12], the tuning characteristic of fo can be modelled, as shown in Fig. 5(b), and the mass and built-in strain of the graphene can be determined. These models yield a mass of approximately 40 times that of intrinsic graphene, and a strain of 2.2%. This mass enhancement is attributed to the same contamination to which we ascribe the mobility reduction.

The small signal electrical model for the device is shown

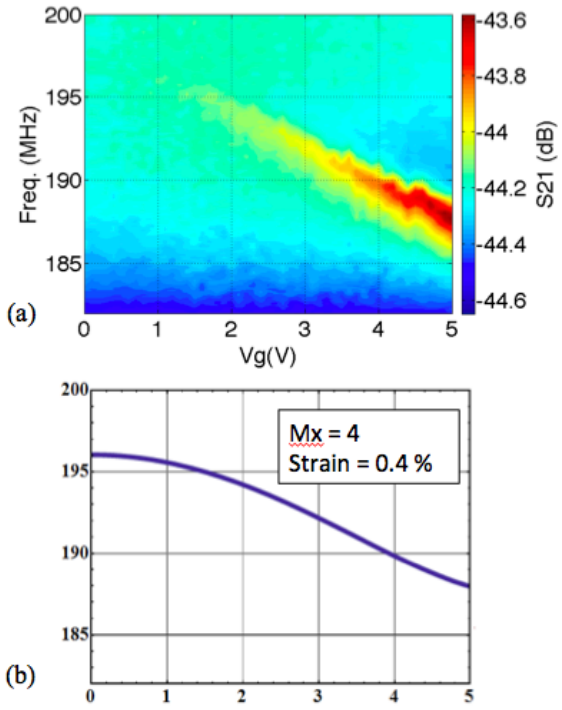

Fig. 6. S_{21} magnitude as a function of frequency and V_{gs}, which demonstrates a greater tuning range due to lower built-in stress from the SU-8 clamp.

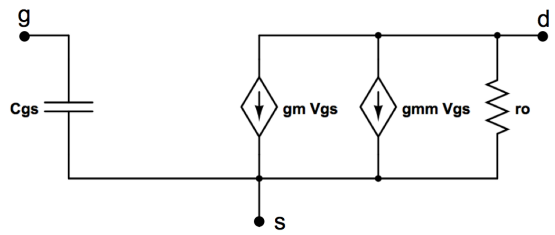

Fig. 7. Small signal electrical model for a GNER.

in Fig. 7. The small signal output current is given by

$$I_d = j\omega C_{tot}\tilde{V}_{gs} - j\omega\frac{\tilde{z}}{z_0}C_g V_{gs} + V_{ds}\frac{dG}{dV_{gs}}\tilde{V}_{gs} - V_{ds}\frac{dG}{dV_{gs}}\frac{\tilde{z}}{z_0}V_{gs} \quad (1)$$

$$\tilde{z} = -\frac{1}{m}\frac{C_g}{z_0}V_g\frac{1}{\omega_0^2 - \omega^2 + \frac{j\omega_0\omega}{Q}}\tilde{V}_{gs} \quad (2)$$

$$g_m = V_{ds}\frac{dG}{dV_{gs}} \quad (3)$$

where C_{tot} is the total capacitance of the device, $\tilde{V}_{gs}$ is the RF voltage amplitude, $\tilde{z}$ is the resonator displacement amplitude, z_0 is the average gate to channel distance, C_g is the gate capacitance, m is the resonator mass, and G is the graphene conductance.

The first two terms in this equation are the feedthrough current and the mechanical displacement current seen in traditional passive MEMS devices [7]. The third term is identical

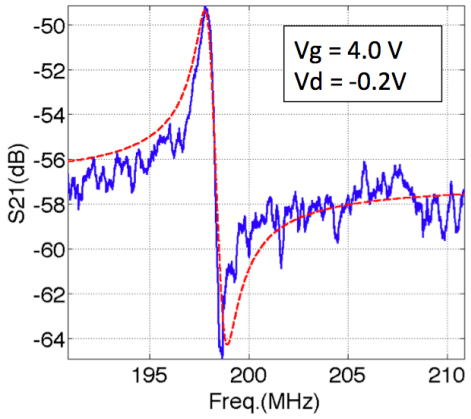

Fig. 8. S_{21} with model fit for a single bias point.

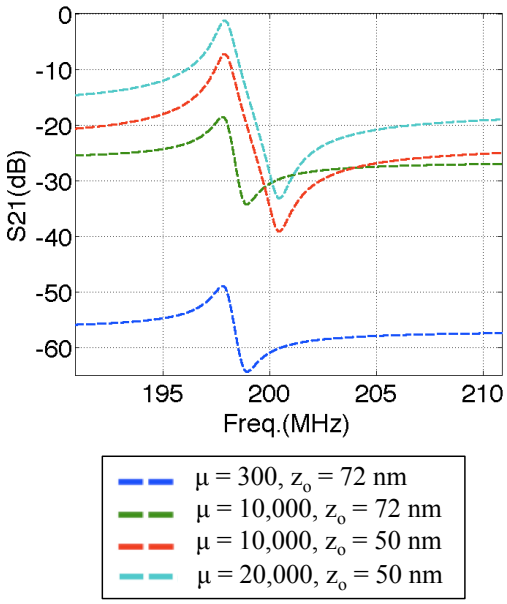

Fig. 9. Projected improvement of GNERs. The bottom trace is identical to the fit in Fig. 8. The other traces are for devices with identical lateral dimensions, but with improved mobility and lower z_0.

to the output current of a typical FET. The fourth term is due to the mechanical motion of the membrane being amplified by the device g_m. Using the extracted mass of the device from Fig 5, and the output current terms given in (4), the S_{21} of the device can be modelled as shown in Fig. 8. This device has a Q of 250 at an f_o of 197.8 MHz. The discrepancy in the model is probably due to capacitive parasitics not accounted for in the model, and spatial nonuniformity in the strain being applied to the graphene.

Fig. 9 shows projections for improved GNER transduction with decreasing z_0, and higher material quality which is reflected in increased μ_{fe}. The bottom trace in the figure is the same fit from Fig. 8. The additional traces are model simulations showing that as mobility is increased to 20,000 cm^2/V-s and z_0 is decreased to 50 nm, the same device may exhibit an IL approaching 0 dB. This IL would make GNERs competitive with existing resonator technologies such as film bulk acoustic resonators (FBARs).

IV. Conclusion

In this work we have shown that the room-temperature Q and f_o of GNERs can be improved by applying additional strain to the graphene membrane using an SU-8 clamp. A small-signal model is presented based on both the electrical and mechanical parameters of the device which shows good agreement with measured data. Although the electrical transport of the graphene used in this study is reduced due to contamination in the fabrication process, projections of resonator performance with improved material quality for a device with similar geometry indicate that GNERs may have IL values that are very comparable with other resonator technologies such as FBARs.

Acknowledgment

The authors like to thank Arend M. van der Zande, Nicholas Petrone, Victor Abramsky, Eugene Hwang, and Changhyuk Lee for critical discussions. Fabrication was performed at the Cornell Nano-Scale Facility, a member of the National Nanotechnology Infrastructure Network, which is supported by the National Science Foundation (Grant ECS-0335765), and Center for Engineering and Physical Science Research (CEPSR) Clean Room at Columba University. The authors acknowledge the support by Qualcomm Innovation Fellowship (QInF) 2012 and AFOSR MURI FA9550-09-1-0705.

References

[1] K. S. Novoselov, A. K. Geim, S. V. Morozov, D. Jiang, Y. Zhang, S. V. Dubonos, I. V. Grigorieva, and A. A. Firsov, "Electric field effect in atomically thin carbon films," *Science*, vol. 306, no. 5696, pp. 666–669, 2004.

[2] C. Lee, X. Wei, J. W. Kysar, and J. Hone, "Measurement of the elastic properties and intrinsic strength of monolayer graphene," *Science*, vol. 321, no. 5887, pp. 385–388, 2008.

[3] I. Meric, M. Y. Han, A. F. Young, B. Ozyilmaz, P. Kim, and K. L. Shepard, "Current saturation in zero-bandgap, top-gated graphene field-effect transistors," *Nature Nanotech.*, vol. 3, no. 11, pp. 654–659, 2008.

[4] C. R. Dean, A. F. Young, I. Meric, C. Lee, L. Wang, S. Sorgenfrei, K. Watanabe, T. Taniguchi, P. Kim, K. L. Shepard, and J. Hone, "Boron nitride substrates for high-quality graphene electronics," *Nature Nanotechnology*, vol. 5, no. 10, pp. 722–726, 2010.

[5] J. S. Bunch, A. M. van der Zande, S. S. Verbridge, I. W. Frank, D. M. Tanenbaum, J. M. Parpia, H. G. Craighead, and P. L. McEuen, "Electromechanical resonators from graphene sheets," *Science*, vol. 315, no. 5811, pp. 490–493, 2007.

[6] C. Chen, S. Rosenblatt, K. I. Bolotin, W. Kalb, P. Kim, I. Kymissis, H. L. Stormer, T. F. Heinz, and J. Hone, "Performance of monolayer graphene nanomechanical resonators with electrical readout," *Nature Nanotechnol.*, vol. 4, pp. 861–867, Dec. 2009.

[7] Y. Xu, C. Chen, V. V. Deshpande, F. A. DiRenno, A. Gondarenko, D. B. Heinz, S. Liu, P. Kim, and J. Hone, "Radio frequency electrical transduction of graphene mechanical resonators," *Applied Physics Letters*, vol. 97, no. 24, p. 243111, 2010.

[8] D. Weinstein and S. A. Bhave, "The resonant body transistor," *Nano Lett.*, vol. 10, no. 4, pp. 1234–1237, 2010.

[9] S. Lee, C. Chen, V. V. Deshpande, G.-H. Lee, I. Lee, M. Lekas, A. Gondarenko, Y.-J. Yu, K. Shepard, P. Kim, and J. Hone, "Electrically integrated su-8 clamped graphene drum resonators for strain engineering," *Applied Physics Letters*, vol. 102, no. 15, p. 153101, 2013.

[10] N. Petrone, C. R. Dean, I. Meric, A. M. van der Zande, P. Y. Huang, L. Wang, D. Muller, K. L. Shepard, and J. Hone, "Chemical vapor deposition-derived graphene with electrical performance of exfoliated graphene," *Nano Lett.*, vol. 12, pp. 2751–2756, June 2012.

[11] H. S. Solanki, S. Sengupta, S. Dhara, V. Singh, S. Patil, R. Dhall, J. Parpia, A. Bhattacharya, and M. M. Deshmukh, "Tuning mechanical modes and influence of charge screening in nanowire resonators," *Phys. Rev. B*, vol. 81, p. 115459, Mar 2010.

[12] W. W. S. Timoshenko, D. H. Young, *Vibration Problems in Engineering*. New York, Wiley, 1974.